Noise Robust Recognition Method Based on Scatterer Pattern for Radar HRRP Data

Hua He, Lan Du, *Member, IEEE*, Penghui Wang, Hongwei Liu, *Member, IEEE*
National Lab. of Radar Signal Processing, Xidian University, Xi'an, China
Email: dulan@mail.xidian.edu.cn

***Abstract*—In this paper, a novel noise-robust recognition method for high-resolution range profile (HRRP) data is proposed based on target scatterer pattern to enhance its recognition performance under the test condition of low SNR. The target dominant scatterers are first extracted based on the scattering center model of complex HRRP data via the orthogonal matching pursuit (OMP) algorithm to realize noise reduction. Then a scatterer matching recognition algorithm based on Hausdorff distance (HD) is developed with the magnitudes and locations of extracted dominant scatterers used as the feature patterns. Experimental results on the measured HRRP data demonstrate that the proposed method can improve the recognition performance under the relatively low SNR condition for both orthogonal and superresolution representations of scattering center model.**

***Index Terms*—Radar automatic target recognition (RATR), high-resolution range profile (HRRP), orthogonal matching pursuit (OMP), point pattern matching, Hausdorff distance**

I. Introduction

Radar high-resolution range profile (HRRP) has received intensive attention from the radar automatic target recognition (RATR) community [1]–[4], [7], [11], [14]. For the RATR problem, the training data are usually collected under the condition of high signal-to-noise ratio (SNR) via some cooperative measurement experiments or directly via simulations; while the test samples are usually got in the non-cooperative circumstance (e.g., at the battle time), where the high SNR condition cannot be guaranteed due to the long distance away from the non-cooperative targets [5], [6], [9], [12]. As shown in the experimental results in [4], the recognition performance dramatically deteriorates under the low test SNR. Therefore, the noise-robustness of a recognition algorithm is very important in the real application.

There are usually three approaches to improve the recognition performance of HRRP data under the low test SNR.

- One is to extract the noise-robust features from the noised HRRP test samples. As discussed in [12], the bispectrum feature of the complex radar signal can suppress additive disturbances that are described by the symmetric probability density functions (pdfs). However, the method above requires a HRRP sequence to get the ensemble average estimation for the bispectrum feature. Such a requirement in the test stage will definitely decrease the recognition speed.
- Another method is to modify the parameters of statistical model in high SNR according to the noise level of the test sample. Based on the additive real-valued noise assumption, [5] proposes a noise-robust modification method for multitask-learning based factor analysis model. Although the good noise robustness is achieved via the proposed method, it suffers from a high computational burden to adaptively modify the parameters related to the SNR level in the statistical model.
- The last but also the most natural choice is to remove the noise component in radar echo before classification. Wavelet shrinkage is proposed as a denoising method for HRRP data in [9]. As shown in the experiments in [9], its performance depends on the approximation-detail threshold setting and degrades largely in the presence of severe noise contamination.

The research reported here seeks a denoising method based on sparse representation of HRRP data and develops a scatterer matching recognition algorithm for the denoised data. The scattering coefficients and locations of the dominant scattering centers are first estimated for a noisy test sample by solving the sparse optimization problem with the noise level constraint, then the scatterer matching algorithm based on Hausdorff distances (HDs) between its dominant scatterers and those from the training templates is used to distinguish the test sample. In the experiments based on measured HRRP dataset, the proposed method shows the inspiring recognition performance under the relatively low SNR condition for both orthogonal and superresolution Fourier dictionaries based sparse representations.

The remainder of the paper is organized as follows. We introduce the scattering center model and denoising method in Section II. The scatterer matching recognition method is developed in Section III-B. The detailed experimental results based on measured HRRP data are provided in Section IV, followed by conclusions in Section V.

II. Denoising Method Based on Sparse Representation

A. Scattering center model for complex HRRP data

According to literature [13], the high-frequency scattering response of an object is well approximated as a sum of responses from individual scattering centers. Thus the discrete

This work was partially supported by the National Science Foundation of China (No.61271024 and No.61322103).

complex frequence responce in baseband is denoted as

$$y(l)=\sum_{n=1}^{K_0}\omega(n)\cdot\exp\left(-j2\pi\frac{2R_n}{c}(l-1)\Delta f\right) \qquad (1)$$

where $y(l)$ represents the lth frequency response with $l\in\{1,\cdots,L\}$ and L denoting the number of frequency components, K_0 is the number of scatterers, R_n denotes the radial distance between the nth scatterer and the radar, Δf denotes the frequency interval between the neighboring frequency components in the discrete frequency response. In (1), the parameters to be estimated are $\{K_0,\{\omega(n),R_n\}_{n=1}^{K_0}\}$.

If we assume that each R_n in (1) is an integer multiple of range resolution ΔR, then (1) can be rewritten as

$$\begin{aligned} y(l) &= \textstyle\sum_{k=1}^{K,r_k\in\{R_n\}_{n=1}^{K_0}} w(k)\cdot\exp\left(-j2\pi\frac{2r_k}{c}(l-1)\Delta f\right)\\ &\quad+\textstyle\sum_{k=1}^{K,r_k\notin\{R_n\}_{n=1}^{K_0}} w(k)\cdot\exp\left(-j2\pi\frac{2r_k}{c}(l-1)\Delta f\right)\\ &= \sum_{k=1}^{K} w(k)\cdot\exp\left(-j2\pi\frac{2r_k}{c}(l-1)\Delta f\right) \end{aligned} \qquad (2)$$

where $\{r_k\}_{k=1}^{K}$ denote the locations of range cells with $K>K_0$ denoting the number of range cells, $w(k)$ represents the corresponding scattering coefficient from the kth range cell. For $r_k=R_{n'}$ with $R_{n'}\in\{R_n\}_{n=1}^{K_0}$, $w(k)=\omega(n')$; otherwise, $w(k)=0$. In this expression (2), K_0 equals to the number of the non-zero elements in vector $\boldsymbol{w}$, and $r_k=k\cdot\Delta R$, then the parameters to be estimated are only $\{w(k)\}_{k=1}^{K}$.

Let

$$\begin{aligned} \boldsymbol{\phi}(r_k) &= \begin{bmatrix} 1,\exp(-j\frac{4\pi}{c}r_k\Delta f),\exp(-j\frac{4\pi}{c}r_k 2\Delta f), \\ \cdots,\exp(-j\frac{4\pi}{c}r_k(L-1)\Delta f) \end{bmatrix}^{\mathrm{T}}\\ \boldsymbol{\Phi} &= [\boldsymbol{\phi}(r_1),\boldsymbol{\phi}(r_2),\cdots,\boldsymbol{\phi}(r_K)] \end{aligned} \qquad (3)$$

Considering the noise component in the real application, the signal model in (2) can be expressed in a vector-matrix form as

$$\boldsymbol{y}=\boldsymbol{\Phi}\boldsymbol{w}+\boldsymbol{\eta} \qquad (4)$$

where $\boldsymbol{y}=[y(1),y(2),\cdots,y(L)]^{\mathrm{T}}$, $\boldsymbol{\eta}=[\eta(1),\eta(2),\cdots,\eta(L)]^{\mathrm{T}}$ represents the noise component, $\boldsymbol{w}=[w(1),w(2),\cdots,w(K)]^{\mathrm{T}}$ denotes the complex HRRP sample, and $|\boldsymbol{w}|$ is the corresponding real HRRP sample. When $K=L$, $\boldsymbol{\Phi}$ is a complete orthogonal basis matrix; when $K>L$, $\boldsymbol{\Phi}$ is a non-orthogonal and redundant dictionary matrix, then the superresolution representation can be achieved.

B. Noise reduction via orthogonal matching pursuit algorithm

According to the scattering center model introduced above, the denoised frequency response can be recovered as $\hat{\boldsymbol{y}}=\boldsymbol{\Phi}\hat{\boldsymbol{w}}$, where $\hat{\boldsymbol{w}}$ denotes the estimated scattering coefficients from the target scatterers. As discussed in [17] for CS-based ISAR imaging, the target signal can be approximated by the echoes from the dominant scattering centers which are assumed to be sparsely distributed in the target, while those from the weak scattering centers are regarded as the noise components. Therefore, $\hat{\boldsymbol{w}}$ can be estimated by solving the following sparse optimization problem

$$\hat{\boldsymbol{w}}=\arg\min_{\boldsymbol{w}}\|\boldsymbol{y}-\boldsymbol{\Phi}\boldsymbol{w}\|_2^2 \qquad \text{s.t. } \|\boldsymbol{w}\|_0=K_0 \qquad (5)$$

where $\|\cdot\|_2$ denotes the l_2 norm, $\|\cdot\|_0$ denotes the l_0 norm and $\|\boldsymbol{w}\|_0=K_0$ represents that there are K_0 non-zero elements in vector $\boldsymbol{w}$.

According to the sparse representation theory [16], if $K_0<(M^{-1}+1)/2$, it is a unique solution of (5). Here M denotes the maximum correlation between the columns in the basis matrix $\boldsymbol{\Phi}$. If K_0 is known as the prior information, the orthogonal matching pursuit (OMP) algorithm [8] can be utilized for (5) to get its approximate solution.

In real application, it is hard to know the number of target scatterers K_0, but the noise power δ in the frequency response from the noised HRRP sample can be estimated via some pre-processing methods. Thus it is reasonable to terminate the OMP algorithm when the residual signal power is lower than the noise power. In this way, the sparse optimization problem should be

$$\hat{\boldsymbol{w}}=\arg\min_{\boldsymbol{w}}\|\boldsymbol{w}\|_0 \qquad \text{s.t. } \|\boldsymbol{y}-\boldsymbol{\Phi}\boldsymbol{w}\|_2^2<\delta \qquad (6)$$

where δ denotes the estimated noise power in the frequency response, $|\hat{\boldsymbol{w}}|$ is the denoised HRRP sample.

III. Scatterer Matching Recognition Method

As discussed in Section II, the target scattering coefficient vector $\hat{\boldsymbol{w}}$ can be learned via the OMP algorithm for a complex HRRP sample. The indices and absolute values of the nonzero entries in $\hat{\boldsymbol{w}}$ indicate the locations and magnitudes of the target scatterers. In the following, we will develop a scatterer matching algorithm with the magnitudes and locations of extracted dominant scatterers used as the feature patterns.

A. Hausdorff distance between point sets

The Hausdorff measure is a well-known method for representing the distance between two point sets without having an a priori correspondence between the two sets [10]. Given the two point sets $\mathbb{A}=\{\boldsymbol{a}_1,\boldsymbol{a}_2,\cdots,\boldsymbol{a}_N\}$ and $\mathbb{B}=\{\boldsymbol{b}_1,\boldsymbol{b}_2,\cdots,\boldsymbol{b}_Q\}$, the Hausdorff distance (HD) is defined as

$$H(\mathbb{A},\mathbb{B})=\max\Big(h(\mathbb{A},\mathbb{B}),h(\mathbb{B},\mathbb{A})\Big) \qquad (7)$$

with

$$h(\mathbb{A},\mathbb{B})=\max_{\boldsymbol{a}_n\in\mathbb{A}}\min_{\boldsymbol{b}_q\in\mathbb{B}}d(\boldsymbol{a}_n,\boldsymbol{b}_q) \qquad (8)$$

where $d(\boldsymbol{a}_n,\boldsymbol{b}_q)$ denotes a distance between pattern vectors $\boldsymbol{a}_n$ and $\boldsymbol{b}_q$. To solve the problem that an outlier or occlusion could skew an otherwise close correspondence, some partial Hausdorff distance (PHD) measures are proposed, of which the least trimmed square Hausdorff distance (LTS-HD) is regarded to be robust [15]. The directed LTS-HD may be written

$$h_{\mathrm{LTS}}(\mathbb{A},\mathbb{B})=\frac{1}{P}\sum_{\boldsymbol{a}_{n_1}\in\mathbb{A}'}\min_{\boldsymbol{b}_q\in\mathbb{B}}d(\boldsymbol{a}_{n_1},\boldsymbol{b}_q) \qquad (9)$$

where $\mathbb{A}'=\{\boldsymbol{a}_1,\boldsymbol{a}_2,\cdots,\boldsymbol{a}_P\}$, $\mathbb{A}'\subset\mathbb{A}$, $P<N$, $\min_{\boldsymbol{b}_q\in\mathbb{B}}d(\boldsymbol{a}_{n_1},\boldsymbol{b}_q)<\min_{\boldsymbol{b}_q\in\mathbb{B}}d(\boldsymbol{a}_{n_2},\boldsymbol{b}_q)$ for each $\boldsymbol{a}_{n_1}\in\mathbb{A}'$

and $\boldsymbol{a}_{n_2} \in \mathbb{A} - \mathbb{A}'$. Thus LTS-HD takes the mean of the P minimum distances between the point sets.

Since scatterer distribution is the important information contained in HRRP data, the locations and magnitudes of the target scatterers can be used as the feature patterns for HRRP target recognition. Let $\mathbb{S}_{\mathbb{A}} = \{s_{\mathbb{A}1}, s_{\mathbb{A}2}, \cdots, s_{\mathbb{A}N}\}$ denote the location indices of scatterers extracted from an HRRP sample and $|\hat{\boldsymbol{w}}_{\mathbb{S}_{\mathbb{A}}}| = [|\hat{w}_{s_{\mathbb{A}1}}|, |\hat{w}_{s_{\mathbb{A}2}}|, \cdots, |\hat{w}_{s_{\mathbb{A}N}}|]^{\mathrm{T}}$ denote the corresponding magnitudes, which are extracted via the OMP algorithm discussed in Section II-B, the feature pattern for each scatterer is $\boldsymbol{a}_n = [s_{\mathbb{A}n}, |\hat{w}_{s_{\mathbb{A}n}}|]^{\mathrm{T}}$ and the point set for this HRRP sample is $\mathbb{A} = \{\boldsymbol{a}_1, \boldsymbol{a}_2, \cdots, \boldsymbol{a}_N\}$, where the pattern order, *i.e.*, the scatterers' order, in $\mathbb{A}$ accord with their extraction order via the OMP algorithm. The scatterers' magnitudes must satisfy $|\hat{w}_{s_{\mathbb{A}1}}| \geq |\hat{w}_{s_{\mathbb{A}2}}| \geq \cdots \geq |\hat{w}_{s_{\mathbb{A}N}}|$. Thus the first extracted scatterers are dominant scatterers for an HRRP sample. As discussed in [17], the target signal can be approximated by the echoes from the dominant scattering centers. We propose a PHD measure, called dominant-scatterers' Hausdorff distance (ds-HD), for our scatterer matching problem. The ds-HD is expressed as

$$
\begin{aligned}
h_{\mathrm{ds}}(\mathbb{A}, \mathbb{B}) &= \frac{1}{P_1} \sum_{\boldsymbol{a}_{n_1} \in \mathbb{A}'} \min_{\boldsymbol{b}_{q_1} \in \mathbb{B}'} d(\boldsymbol{a}_{n_1}, \boldsymbol{b}_{q_1}) \ , \\
h_{\mathrm{ds}}(\mathbb{B}, \mathbb{A}) &= \frac{1}{P_2} \sum_{\boldsymbol{b}_{q_1} \in \mathbb{B}'} \min_{\boldsymbol{a}_{n_1} \in \mathbb{B}'} d(\boldsymbol{b}_{q_1}, \boldsymbol{a}_{n_1})
\end{aligned} \tag{10}
$$

In (10), $\mathbb{A}' = \mathbb{A}'_1 \cup \{\boldsymbol{a}_{P_1}\} = \{\boldsymbol{a}_1, \boldsymbol{a}_2, \cdots, \boldsymbol{a}_{P_1 - 1}\} \cup \{\boldsymbol{a}_{P_1}\}$, $\mathbb{A}' \subset \mathbb{A}$, $P_1 < N$, $\|\boldsymbol{\Phi}\hat{\boldsymbol{w}}_{\mathbb{S}_{\mathbb{A}'_1}}\|_2 < r\|\boldsymbol{y}_{\mathbb{A}}\|_2$ and $\|\boldsymbol{\Phi}\hat{\boldsymbol{w}}_{\mathbb{S}_{\mathbb{A}'}}\|_2 \geq r\|\boldsymbol{y}_{\mathbb{A}}\|_2$ with $\boldsymbol{y}_{\mathbb{A}}$ denoting the frequency response of the HRRP sample corresponding to $\mathbb{A}$ and $0 < r < 1$. Thus $\mathbb{A}'$ represents the dominant scatterers' pattern set of the HRRP sample. Similarly for $\mathbb{B}'$. The parameter r is determined via the cross-validation method in the classification experiment. The ds-HD is the mean of distances between the dominant scatterers from two point sets. The PHD used in this paper is defined as

$$
H(\mathbb{A}, \mathbb{B}) = \max\Big(h_{\mathrm{ds}}(\mathbb{A}, \mathbb{B}), h_{\mathrm{ds}}(\mathbb{B}, \mathbb{A})\Big) \tag{11}
$$

The $d(\cdot, \cdot)$ in (10) is calculated from the Mahalanobis distance

$$
d(\boldsymbol{a}_{n_1}, \boldsymbol{b}_{q_1}) = \sqrt{(\boldsymbol{a}_{n_1} - \boldsymbol{b}_{q_1})^{\mathrm{T}} \boldsymbol{\Sigma}^{-1} (\boldsymbol{a}_{n_1} - \boldsymbol{b}_{q_1})} \tag{12}
$$

where $\boldsymbol{\Sigma}$ is a diagonal matrix, its diagonal entries are the measurement error variances of each feature in the feature vectors in the point sets. Here one feature in our pattern is the location index of a scatterer, while the other is the intensity of the scatterer.

B. HRRP recognition algorithm based on scatterer matching

As discussed in [2]–[5], [7], [11], [14], HRRPs from complex targets yield target signatures that are a strong function of the target-sensor orientation, referred to as target-aspect sensitivity in [3], [4]. To deal with the target-aspect sensitivity, the multi-aspect HRRP dataset from each target is divided into subsets (as in [3], [4]), where the HRRP data in each subset are collected from a target-aspect sector roughly without the scatterers' motion through range cells (MTRC). Thus each subset is defined to be an aspect-frame from the target [3], [4]. For each aspect-frame from the training data, we use the HRRP sample with the smallest summation of PHDs between it and each other samples in this aspect-frame as the frame template. In the classification stage, the denoising processing is implemented for a single test sample. Then according to the nearest neighbor criterion, the class membership of the test sample will be assigned to the class of the frame template with the minimum PHD. In this paper, to deal with the time-shift sensitivity and amplitude-scale sensitivity,each training or test sample is time-shift compensated with its first geometric moment and normalized by dividing its l_2-norm.

IV. Experimental Results

We examine the performance of the proposed model on the measured airplane data used in [3]–[5]. The center frequency and bandwidth of the radar are $5520MHz$ and $400MHz$. The projections of target trajectories onto the ground plane are shown in Figure 1. In order to test the generalization performance of the recognition methods, the 2nd and the 5th segments of Yak-42, the 6th and the 7th segments of Cessna, the 5th and the 6th segments of An-26 are taken as the training samples, other data segments are taken as test samples in our experiments.

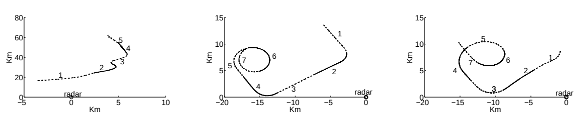

(a) (b) (c)

Fig. 1. Projections of target trajectories onto the ground plane: (a) Yak-42; (b) Cessna Citation S/II; (c) An-26.

This HRRP dataset is measured under high SNR (≈ 40dB) and without any interference. In order to evaluate the denoising performance of our proposed method, we add simulated white noises to the inphase and quadrature components of the complex frequency responses from the test samples. The SNR is defined as

$$
\mathrm{SNR} = 10 \times \log_{10}\left(\frac{\sum_{l=1}^{L} P_{y_l}}{L \times P_{\mathrm{Noise}}}\right) \tag{13}
$$

where P_{y_l} denotes the power of the lth frequency response from the original test sample, L denotes the number of frequency components (here $L = 256$), and P_{Noise} denotes the power of noise in each frequency component.

Firstly, we show the denoising results on the measured data. Figure 2 gives the three denoising examples for HRRP data under SNR=10dB via OMP with $K = 2 \times L$. Comparing between the original HRRP, noisy HRRP and denoised HRRP samples, we can see that the proposed denoising method works well not only in removing the noise component but also in reconstructing the target scattering coefficients.

To quantificationally evaluate the denoising performance, we define the relative HD-based-error as

$$
E = \frac{H(\hat{\mathbb{A}}, \bar{\mathbb{A}})}{H(\bar{\mathbb{A}}, \{[0, 0]^{\mathrm{T}}\})} \tag{14}
$$

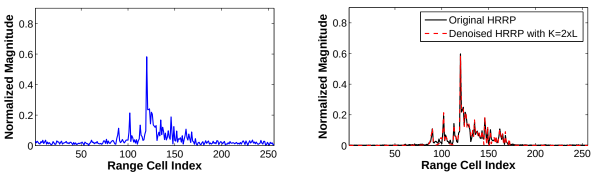

(a)

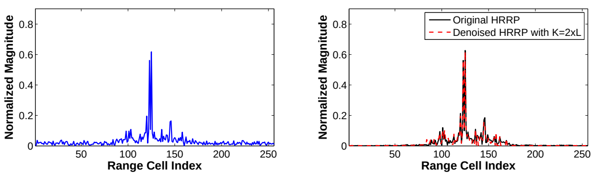

(b)

Fig. 2. Denoising examples for three measured HRRP samples. Left column: the noisy HRRP samples under SNR=10dB; Right column: the original HRRPs under high SNR about 40dB (black real lines) and the denoised HRRPs from those on the left via OMP with $K = 2 \times L$ (red dot lines).

where $\hat{\mathbb{A}}$ denotes the point set for the denoised HRRP sample, $\bar{\mathbb{A}}$ denotes the point set for the original HRRP sample without noise, $H(\cdot, \cdot)$ is calculated according to (11), and the denominator $H(\bar{\mathbb{A}}, \{[0, 0]^{\mathrm{T}}\})$ is used to normalize the HD-based-error. Figure 3 further quantitatively depicts the denoising performance for all test HRRP samples in our data set via the average relative HD-based-errors. Here the relative HD-based-error for each test sample is calculated according to (14) with $\bar{\mathbb{A}}$ denoting the point set for the original HRRP samples under SNR≈40dB. We also use five noisy datasets with different adding noise processing to evaluate the robustness of our proposed method. As shown in Figure 3, the average relative HD-based-errors of the denoised HRRP data are smaller than those of the noisy data, especially under the low SNR conditions.

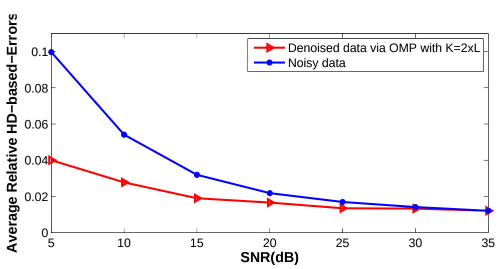

Fig. 3. Variation of the average relative HD-based-errors for all test HRRP samples in our data set with SNR. The blue line denotes the average relative errors between the noisy data and the original data under high SNR about 40dB, while the red line denotes those between the denoised data via OMP with $K = 2 \times L$ and the original data under high SNR about 40dB. The errors are averaged over five runs with different adding noise processing.

Then in the classification experiment, we compare the proposed noise-robust scatterer matching recognition method with its non-robust version and the existing statistical recognition method based on Gaussian model [11], [14] without denoising. Figure 4 shows the average recognition rates of our measured dataset versus SNR. The non-robust version of scatterer matching recognition method means the noise power threshold δ for a test sample is very small, which accords to a high SNR case (≈40dB) and does not equal to its real value. In this way, the noised scatterer information is used in the following HD-based recognition method. As shown in Figure 4, when the SNR≥25dB, the influence of noise is not so significant, the four methods yield the similar recognition accuracies, and the Gaussian model is a little better than other methods only under SNR≈ 30dB; when SNR≤25dB, the two noise-robust methods outperform the noised Gaussian model and noised HD-based method, and the performance of our superresolution version ($K = 2 \times L$) is a little better than that of the orthogonal version ($K = L$). In the real application, we need a threshold of the recognition rate for the RATR problem to evaluate the noise-robustness performance. According to our experience and some papers based on our measured data from the three real airplanes [3]–[5], [7], recognition rate larger than 80% can satisfy the requirement of the real application. As shown in Figure 4, if we assume the recognition rate threshold is 80%, our method with $K = 2 \times L$ can work under the test condition of SNR≥18dB, while the noised Gaussian model requires SNR≥24dB. According to the radar equation, in the real application a 1dB advantage in SNR will bring an increase about 6% in the recognition distance between radar and target. Therefore, the recognition distance of our proposed method is about 1.42 times as long as that of the noised Gaussian model.

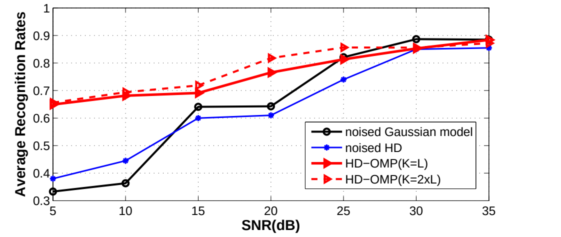

Fig. 4. Variation of the average recognition rates with SNR via statistical recognition based on Gaussian model [11], [14] without denoising, HD-based scatterer matching recognition without denoising for test samples and with test samples denoised via OMP ($K = L$ and $K = 2 \times L$). The recognition rates are averaged over five runs with different adding noise processing.

V. Conclusion

A noise-robust scatterer matching recognition method is proposed for radar HRRP data in this paper. The target dominant scatterers in noisy HRRP data are first extracted via the OMP algorithm, and then the magnitudes and locations of extracted scatterers are used as the feature patterns in the scatterer matching recognition algorithm based on HD. Experimental results on the synthetic and measured data show that the proposed method can obtain good recognition and denoising performances under the relatively low test SNR condition. In the real application, the SNR advantage can effectively extend the recognition distance between the target and radar.

REFERENCES

[1] B. Chen, H. W. Liu, J. Chai, and Z. Bao, “Large margin feature weighting method via linear programming,” *IEEE Transactions on Knowledge and Data Engineering*, vol. 21(10), pp. 1475–1488, 2009.

[2] K. Copsey and A. R. Webb, “Bayesian Gamma mixture model approach to radar target recognition,” *IEEE Transactions on Aerosp. Electron. Syst.*, vol. 39(4), pp. 1201–1217, 2003.

[3] L. Du, H. W. Liu, and Z. Bao, “Radar HRRP statistical recognition: parametric model and model selection,” *IEEE Transactions on Signal Processing*, vol. 56(5), pp. 1931–1944, 2008.

[4] L. Du, H. W. Liu, Z. Bao, and J. Y. Zhang, “A two-distribution compounded statistical model for radar HRRP target recognition,” *IEEE Transactions on Signal Processing*, vol. 54(6), pp. 2226–2238, 2006.

[5] L. Du, H. W. Liu, P. H. Wang, B. Feng, M. Pan, and Z. Bao, “Noise robust radar HRRP target recognition based on multitask factor analysis with small training data size,” *IEEE Transactions on Signal Processing*, vol. 60(7), pp. 3546–3559, 2012.

[6] L. Du, Y. Ma, B. S. Wang, and H. W. Liu, “Noise-robust classification of ground moving targets based on time-frequency feature from micro-Doppler signature,” *IEEE Sensors Journal*, vol. 14(8), 2014.

[7] L. Du, P. H. Wang, H. W. Liu, M. Pan, F. Chen, and Z. Bao, “Bayesian spatiotemporal multitask learning for radar HRRP target recognition,” *IEEE Transactions on Signal Processing*, vol. 59(7), pp. 3182–3196, 2011.

[8] M. Elad, *Sparse and Redundant Representations: From Theory to Applications in Signal and Image Processing*, 3rd ed. New York: Springer, 2011.

[9] B. M. Huether, S. C. Gustafson, and R. P. Broussard, “Wavelet preprocessing for high range resolution radar classification,” *IEEE Transactions on Aerosp. Electron. Syst.*, vol. 37(4), 2001.

[10] D. P. Huttenlocher, G. A. Klanderman, and W. J. Rucklidge, “Comparing images using the Hausdorff distance,” *IEEE Trans. Patt. Anal. Machine Intell.*, vol. 15, p. 850C863, 1993.

[11] S. P. Jacobs, “Automatic target recognition using high-resolution radar range profiles,” Ph.D. dissertation, Washington University, 1999.

[12] L. Jouny, F. D. Garber, and R. L. Moses, “Radar target identification using the bispectrum: a comparative study,” *IEEE Transactions on Aerosp. Electron. Syst.*, vol. 31(1), 1995.

[13] J. B. Keller, “Geometrical theory of diffraction,” *J. Opt. Soc. Amer.*, vol. 52, pp. 116–130, 1962.

[14] R. A. Mitchell and J. J. Westerkamp, “Robust statistical feature based aircraft identification,” *IEEE Transactions on Aerosp. Electron. Syst.*, vol. 35(3), pp. 1077–1094, 1999.

[15] D.-G. Sim, O.-K. Kwon, and R.-H. Park, “Object matching algorithms using robust Hausdorff distance measures,” *IEEE Transactions on Image Processing*, vol. 8(3), pp. 425–429, 1999.

[16] M. B. Zadeh and C. Jutten, “On the stable recovery of the sparsest overcomplete representations in the presense of noise,” *IEEE Transactions on Signal Processing*, vol. 58(10), pp. 5396–5400, 2010.

[17] L. Zhang, M. D. Xing, C. W. Qiu, J. Li, J. L. Sheng, Y. C. Li, and Z. Bao, “Resolution enchancement for inversed synthetic aperture radar imaging under low SNR via improved compressive sensing,” *IEEE Transactions on Geoscience and Remote Sensing*, vol. 48(10), pp. 3824–3838, 2010.